

ARTICLE

Multimodular vascularized bone construct comprised of vasculogenic and osteogenic microtissues

Nicholas G. Schott  | Huy Vu | Jan P. Stegemann

Department of Biomedical Engineering,
University of Michigan, Ann Arbor,
Michigan, USA

Correspondence

Jan P. Stegemann, Department of Biomedical Engineering, University of Michigan, Ann and Robert H. Lurie Biomedical Engineering Bldg, 1101 Beal Ave, Ann Arbor, MI, 48109, USA.
Email: jpesteg@umich.edu

Funding information

National Institute of Arthritis and Musculoskeletal and Skin Diseases; National Institutes of Health

Abstract

Bioengineered bone designed to heal large defects requires concomitant development of osseous and vascular tissue to ensure engraftment and survival. Adult human mesenchymal stromal cells (MSC) are promising in this application because they have demonstrated both osteogenic and vasculogenic potential. This study employed a modular approach in which cells were encapsulated in biomaterial carriers (microtissues) designed to support tissue-specific function. Osteogenic microtissues consisting of MSC embedded in a collagen-chitosan matrix; vasculogenic (VAS) microtissues consisted of endothelial cells and MSC in a fibrin matrix. Microtissues were precultured under differentiation conditions to induce appropriate MSC lineage commitment, and were then combined in a surrounding fibrin hydrogel to create a multimodular construct. Results demonstrated the ability of microtissues to support lineage commitment, and that preculture primes the microtissues for the desired function. Combination of osteogenic and vasculogenic microtissues into multimodular constructs demonstrated that osteogenic priming resulted in sustained osteogenic activity even when cultured in vasculogenic medium, and that vasculogenic priming induced a pericyte-like phenotype that resulted in development of a primitive vessel network in the constructs. The modular approach allows microtissues to be separately precultured to harness the dual differentiation potential of MSC to support both bone and blood vessel formation in a unified construct.

KEYWORDS

bone tissue engineering, mesenchymal stromal cells, vascularization

1 | INTRODUCTION

Cell-based tissue engineering is being developed as an approach to the repair and regeneration of large and recalcitrant bone defects. (Forrestal et al., 2017) This strategy avoids key drawbacks associated with current autologous tissue grafting, such as donor-site morbidity,

infection, and postoperative chronic pain. (Dimitriou et al., 2011; Laurencin et al., 2006) Orthopedic tissue engineering approaches generally involve the combination of bone-forming cells, inductive factors, and suitable biomaterials to form an orthobiologic construct capable of supporting bone tissue development. Such cell-based strategies have shown clear regenerative potential in animal models,

This is an open access article under the terms of the Creative Commons Attribution-NonCommercial License, which permits use, distribution and reproduction in any medium, provided the original work is properly cited and is not used for commercial purposes.

© 2022 The Authors. *Biotechnology and Bioengineering* published by Wiley Periodicals LLC.

and a smaller number have progressed to clinical trials. (Ho-Shui-Ling et al., 2018) Despite this demonstrated potential, the lack of adequate and timely vascularization has been shown to compromise cellular survival of tissue engineered constructs, and has been identified as a main challenge preventing their clinical translation. (Novosel et al., 2011) This has motivated alternative approaches involving the creation of preformed vascular networks within engineered constructs in vitro, which are designed to accelerate the vascularization process through inosculation with host vasculature upon transplantation. Prevascularized scaffolds have been shown to survive in vivo (Friend et al., 2020; Mishra et al., 2016) and enhance neovascularization in critical-sized cranial defect animal models. (Perry et al., 2019; Roux et al., 2018) Therefore, the development of a vascularized bone construct serves as an attractive means to circumvent challenges with insufficient vascularization and ultimately enable the regenerative potential of cell based strategies for large, complicated osseous defects.

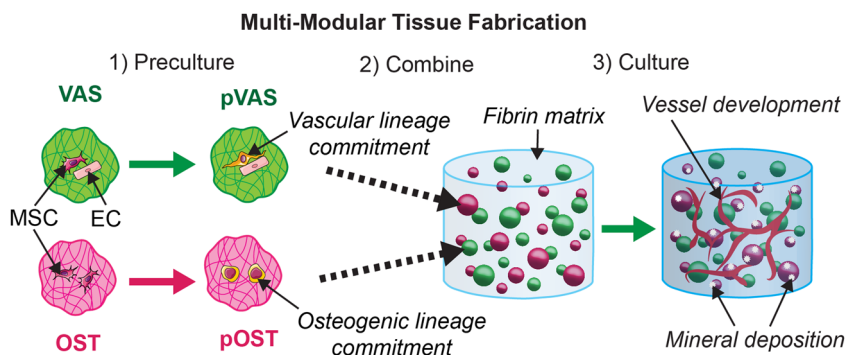
Adult mesenchymal stromal cells (MSC) are extensively used in orthopedic tissue engineering because of their central role in native bone regeneration, ease of isolation and in vitro expansion, and well-documented capacity to undergo controllable osteogenesis both in vitro and in vivo. (Forrestal et al., 2017; Oryan et al., 2017; Schott et al., 2021) MSC are also widely used as supportive pericytes in vascular tissue engineering, in which they play an instrumental role in the process of vessel formation by secreting angiogenic factors and directly interacting with endothelial cells (EC) to stabilize vasculature. (Rohringer et al., 2014; Sears & Ghosh, 2020; Stapor et al., 2014) However, a critical parameter that must be considered to enable the regenerative ability of MSC is their phenotype upon transplantation. Undifferentiated MSC have been shown to secrete soluble factors that directly inhibit osteogenic differentiation in vitro. (Santos et al., 2015) This has motivated efforts to preculture MSC under osteogenic conditions before transplantation to induce appropriate lineage commitment and prevent this repressive effect. This priming strategy has been shown to significantly enhance the bone-forming capacity of MSC in bone defect models. (Annamalai et al., 2019; Wise et al., 2016; Ye et al., 2012) The differentiated state of MSC supporting vascular development is also a matter of consideration as similar inhibitory effects have been shown when combining osteogenically-primed MSC within a vascular matrix comprised of EC and undifferentiated MSC, suggesting the need for pericyte

lineage commitment. (Rao et al., 2015) These findings have motivated research efforts to focus on culturing strategies to achieve appropriate MSC phenotype commitment and enable their regenerative potential for creating vascularized bone constructs.

MSC require a defined set of cues to induce either an osteogenic or pericyte-like phenotype. Osteogenic differentiation of MSC in vitro is often achieved through a period of culture with inductive media containing dexamethasone, ascorbic acid, and β -glycerophosphate. (Jaiswal et al., 1997; Vater et al., 2011) Induction of a pericyte-like lineage in MSC typically involves coculture with EC in vasculogenic medium, and it has been suggested that direct cellular contact with EC is a critical stimulus to induce pericyte differentiation of MSC (Loibl et al., 2014). A range of relatively complex coculturing platforms have been developed to simultaneously support both phenotypic outcomes, most of which employ a "hybrid" culture environment consisting of a mixture of osteogenic and vasculogenic culture media. (Chiesa et al., 2020; Correia et al., 2014; Hutton et al., 2013; Wenz et al., 2018) However, recent work from our group has highlighted challenges with this approach, as osteogenic and vasculogenic medium significantly impair vessel development and osteogenic activity, respectively. (Schott & Stegemann, 2021) These findings are consistent with other work revealing challenges inducing osteogenic differentiation and vessel development simultaneously in hybrid culture media. (Kolbe et al., 2011) These incompatible culture environments makes the concomitant development of osteogenic and vasculogenic tissues a challenge, and motivates alternative strategies for inducing appropriate MSC lineage commitment.

The goal of this study was to generate an MSC-based system capable of promoting simultaneous osteogenic and vasculogenic tissue development. A modular approach was used, in which discrete, cell-laden biomaterial carriers (microtissues) were separately precultured under defined differentiation conditions and were subsequently combined to form a multimodular construct, as shown schematically in Figure 1. The process used to create microtissues allows tailoring of the matrix composition and culture conditions to promote differentiation toward a desired tissue type. In the current study, distinct populations of osteogenic and vasculogenic microtissues were fabricated and precultured to support an osteogenic or pericyte-like phenotype of MSC, respectively. Osteogenic (OST) microtissues used a chitosan-collagen type 1 composite matrix designed to mimic the native bone matrix while providing

FIGURE 1 Overview of multimodular strategy. Schematic diagram of the multimodular approach to creating engineered tissue constructs with both osteogenic and vasculogenic functions (not to scale).



osteoconductive cues. (Barrère et al., 2008; Shoulders & Raines, 2009) Vasculogenic (VAS) microtissues used a fibrin matrix to support cellular remodeling and vessel development. (Rohringer et al., 2014) Our previous work has demonstrated utility for OST and VAS microtissues in supporting bone regeneration (Annamalai et al., 2019) and vascularization (Friend et al., 2020), respectively. In this study, both microtissue types were precultured to induce appropriate MSC lineage commitment and subsequently combined to evaluate the ability of simultaneous osteogenic and vascular tissue development as a proof-of-concept for a multimodular vascularized bone construct.

2 | MATERIALS AND METHODS

2.1 | Cell culture

Human bone marrow-derived mesenchymal stromal cells (MSC; RoosterBio, Inc.) were expanded following the manufacturer's protocol using a high performance hMSC basal medium (SU005) and booster supplements (GTF-SE003). Primary human umbilical vein endothelial cells (EC; Lonza, Inc.) were expanded in fully supplemented Vasculife EC culture medium (VL; Lifeline Cell Technology). Both cell types were cultured in T-175 flasks to 80% confluency and used in experiments between passages 2 and 4. Cells were maintained at 37°C in standard cell culture incubators with media changes every 2 days.

2.2 | Fabrication of microtissues

Microtissues were fabricated using a water-in-oil emulsification process, as previously described. (Annamalai et al., 2019; Friend et al., 2020) A schematic of the overall process is shown in Figure 2a. Osteogenic (OST) and vasculogenic (VAS) microtissues varied in

terms of cellular and matrix composition, outlined in Figure 2b. Before emulsification, 75 ml of 100 cSt polydimethylsiloxane (PDMS) oil (Clearco Products Co. Inc.) was placed into a 100 ml beaker and left on ice. Cells were suspended in a solubilized matrix (2.0 million cells/ml) to make a 6 ml batch of a cell-hydrogel mixture. The mixture was then dispensed into the PDMS bath and mixed by a dual radial-blade impeller at 600 rpm for 5 min to allow for emulsion. Afterwards, the bath temperature was increased to 37°C and emulsion mixture was stirred for an additional 25 min to achieve full gelation. Density separation was used to isolate formed microtissues from the PDMS solution with the addition of phosphate buffer saline (PBS) with 0.1% (v/v) L101 surfactant (BASF) for inversion mixing, followed by 3 centrifugation steps (200g for 5 min each). PDMS was removed after each centrifugation step.

Osteogenic (OST) microtissues comprised of a chitosan-collagen composite hydrogel containing MSC. Fabrication involved suspending MSC within a mixture of solubilized chitosan (75%–85% deacetylated, low molecular weight, ~120 kDa, Sigma), type-1 collagen (MP Biomedicals Inc.), β -glycerophosphate (58.0 wt% in water; Sigma), and glyoxal (68.9 mM in water; Sigma). All stock solutions were kept on ice before microtissue fabrication. Chitosan stock solution was made by suspending 0.25 g of chitosan in 25 ml of water and autoclaving at 121°C for 30 min. Then, 30 μ l glacial acetic acid (17.4 M) was added to the cooled suspension under sterile conditions. The resulting solution (1.0 wt% chitosan in 0.02 N acetic acid) was stirred for 7 days at room temperature and centrifuged at 10 Kg to remove undissolved debris before microtissue fabrication. Collagen stock solution was prepared by dissolving 250 mg of lyophilized collagen in 62.5 ml sterile filtered 0.02 N acetic acid. The resulting solution (0.4 wt% collagen in 0.02 N acetic acid) was stirred 100–200 rpm for 7 days at 4°C. For each 6 ml batch of microtissues, 3 ml collagen type-1 stock (2.0 mg/ml final), 1.5 ml chitosan stock (2.0 mg/ml final), 70 μ l glyoxal (2.0 mM final), and 730 μ l β -glycerophosphate (70.5 mg/ml final) were added and mixed thoroughly. Finally, 700 μ l of cell suspension (2.0 million cells/ml

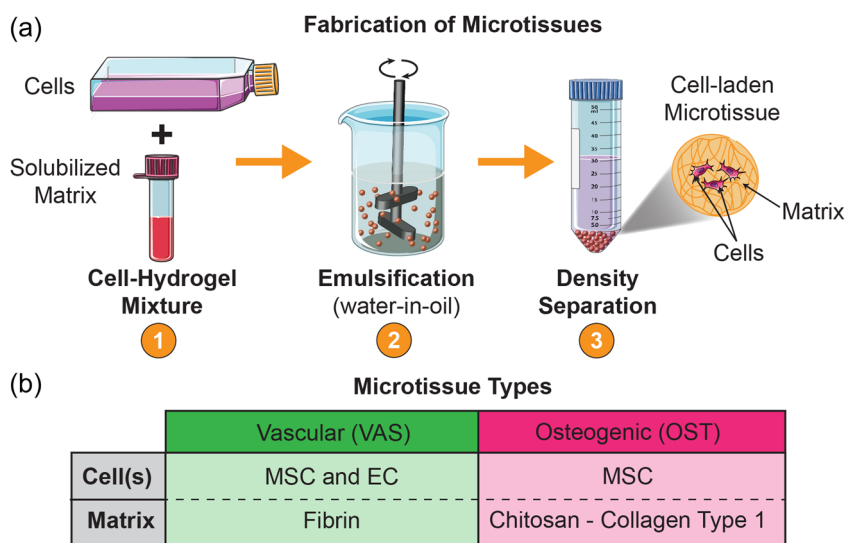


FIGURE 2 Fabrication and composition of microtissues. (a) Schematic overview of the microtissue fabrication and collection process. (b) Composition of osteogenic and vasculogenic microtissues.

microtissues final) was added and mixed thoroughly to the neutralized mixture before emulsification.

Vasculogenic (VAS) microtissues comprised of a fibrin hydrogel containing MSC and EC (1:1 cell ratio). Fabrication involved suspending MSC and EC in a mixture of fibrinogen (Sigma Aldrich), fetal bovine serum (FBS, Corning), and thrombin (50.0 U/ml; Sigma). All stock solutions were kept on ice before microtissue fabrication. Fibrinogen stock solution was prepared by dissolving lyophilized powder in PBS (4.0 mg/ml clottable protein) and sterile filtering. For each 6 ml batch of microtissues, 1.53 ml cell suspension (containing 765 μ l of each cell type, 2 million cells total/ml microtissues final), 600 μ l FBS (10% v/v final), 120 μ l thrombin (1 U/ml final), and 3.75 ml fibrinogen stock solution (2.5 mg/ml final clottable protein) were added and mixed thoroughly before emulsification.

2.3 | Preculture and culture of microtissues and modular constructs

VAS and OST microtissues were separately precultured in suspension using vented conical tubes (CELLTREAT). VAS microtissues were suspended in vasculogenic medium (VL; VascuLife) and OST microtissues in osteogenic differentiation medium (ODM). ODM comprised of Dulbecco's Modified Eagle's Medium (DMEM) containing ascorbic acid-2 phosphate (0.2 mM, Sigma), β -glycerophosphate (10 mM; Sigma), dexamethasone (100 nM; Sigma), and FBS (10% v/v final). Media was changed every 2 days using centrifugation (200g for 5 min) and careful aspiration to avoid losing microtissues.

For assessment of tissue-specific function, culture of VAS and OST microtissues was performed by embedding each microtissue type in a bulk fibrin carrier gel to form a microtissue-laden construct. VAS- or OST-laden constructs were cultured in VL and ODM, respectively. Dulbecco's Modified Eagle's Medium (DMEM; Invitrogen) with 10% FBS was used as control medium (Ctrl) when assessing the vessel-forming and osteogenic capacity of microtissues. Each construct was 500 μ l in volume. Constructs containing VAS or OST microtissues were seeded with 0.25 million cells-worth of each respective microtissue type. Multimodular constructs, embedded with VAS and OST microtissues, contained 0.5 million cells total (0.25 million cells-worth of VAS + 0.25 million cells-worth of OST) and were cultured in VL.

Fabrication of constructs containing either one or multiple microtissue types involved suspending precultured or newly fabricated microtissues in a mixture of fibrinogen, FBS, and thrombin. All stock solutions were kept on ice before construct fabrication. Fibrinogen stock solution was prepared by dissolving lyophilized powder in PBS (4.0 mg/ml clottable protein) and sterile filtering. Batches of microtissues in bulk fibrin gel carriers would be made 2 ml at a time. For each batch, 510 μ l of microtissues (containing 2.0 million cells), 200 μ l FBS (10% v/v final), 40 μ l thrombin (1.0 U/ml final), and 1.25 ml fibrinogen stock solution (2.5 mg/ml final clottable protein) were added and mixed thoroughly. Three constructs (500 μ l each) would be cast per batch into individual wells of a

24-well plate. The plate was then incubated for 30 min at 37°C to facilitate complete gelation of the bulk carrier gel. Each construct received 0.5 ml of appropriate media and changed every 2 days.

A method modified from a previously published study (Friend et al., 2020) was used to achieve desired cell numbers per construct. Briefly, microtissue pellets from each batch were resuspended in 2.0 ml of DMEM and transferred into vented 15 ml conical tubes with filters (CELLTREAT). One hundred microliters of the microtissue suspension would be transferred to a 96-well plate. An equal volume (100 μ l) of an appropriate digestion solution was then added on top of the suspension and mixed. Digestion solutions consisted of collagenase type 1 (1.0 mg/ml in PBS; MP Biomedicals) for OST microtissues and nattokinase (1.0 mg/ml in PBS containing 1.0 mM EDTA (Carrion et al., 2014), Japan Bio Science Laboratory Co., Ltd.) for VAS microtissues. The plate was incubated for 30 min at 37°C to facilitate enzyme activity and microtissue degradation. Cells suspended in the solubilized matrix were then counted using a hemocytometer and used to calculate cell density per microtissue volume. The final volume of the microtissue suspension was then adjusted to provide appropriate cell numbers per construct.

2.4 | Osteogenic marker analysis

Intracellular alkaline phosphatase (ALP) activity, calcium deposition, and DNA content were quantified to assess osteogenic function. Intracellular ALP activity was quantified using a p-nitrophenol phosphate assay (Sigma). Each construct was centrifuged at 10 Kg for 5 min to remove excess media within the hydrogel. After aspirating the supernatant, 500 μ l of PBS containing Triton-X100 (0.5% v/v; Sigma) was added to permeabilize cell membrane and generate a cell lysate solution. Three freeze thaw cycles were performed with brief vortexing in between to facilitate intracellular ALP harvest. Standard curves were constructed using serial dilutions of p-Nitrophenol standard solution (Sigma; N7660) in a 2.0 N NaOH solution. Assay was performed in a clear 96-well plate, where 200 μ l of appropriate standard solution and 10 μ l of cell lysate sample was added to each appropriate well in triplicate. Then, 100 μ l working solution was added to each sample-well. Working solution comprised of 1 ALP substrate tablet (Sigma; N2765) dissolved in 15 ml Alkaline Buffer Solution (Sigma). After 30 min incubation period at 37°C, 90 μ l of 2.0 N NaOH was added to each sample-well to stop reactions and absorbance was read at 405 nm.

DNA content was quantified using a DNA assay kit (Quant-iT™ PicoGreen dsDNA kit; Invitrogen) following the manufacturer's protocol. Same cell lysate solution from the ALP assay was used for DNA quantification. Standard curves were constructed using serial dilutions of λ DNA standard (Invitrogen; 25250) in a 10 mM Tris-HCl solution (pH 7.5). Assay was performed in a black 96-well plate, where 100 μ l of 10 mM Tris-HCl was added to each well. Samples and standards were added in triplicate at 10 μ l per well. Then, 110 μ l of PicoGreen buffer was added to each well, covered in foil and incubated for 30 min at 37°C. Buffer was made by 200-fold

dilution of Quant-iT PicoGreen dsDNA Reagent (ThermoFisher; P11495) in 10 mM Tris-HCl. Following incubation, the plate was read at an excitation of 498 nm and emission of 518 nm.

Calcium deposition was quantified using the orthocresolphthalein complex one (OCPC) method as previously described. (Schott & Stegemann, 2021) Briefly, samples were digested by adding 500 μ l of 1.0 N acetic acid to each sample and incubating overnight at 37°C. To facilitate digestion, constructs were sonicated for 5 s at 10% magnitude. Standard curves were constructed using serial dilutions of CaCl₂ (Sigma) dissolved in 1.0 N acetic acid. Assay was performed using a clear 96-well plate, where 20 μ l of samples and standards were added to respective wells in triplicate. Then, 250 μ l of working solution, consisting of 0.05 mg/ml OCPC in ethanolamine-boric acid-8-hydroxyquinoline buffer, was added to each well. After 10 min of incubation at room temperature, absorbance was measured at 575 nm.

2.5 | Vessel quantification

Vessel network density was quantified to assess vasculogenic capacity of microtissues in culture. Before embedding, microtissues were incubated in a solution of FITC-labeled fibrinogen (1:100 in DMEM) for 30 min at 37°C to provide a fluorescent shell and help discriminate microtissues from the surrounding bulk matrix. At each week throughout culture, constructs were rinsed with PBS (X3 for 5 min each) and fixed using 500 μ l aqueous buffered zinc formalin (Z-fix; Fisher) per gel for 30 min at room temperature. After removal of fixative and another PBS rinse (X3 for 5 min each), constructs were stained with 250 μ l of stain solution comprised of PBS, *Ulex Europaeus* Lectin 1 (UEA; Vector Laboratories; 1:100), and 4', 6-diamidino-2-phenylindol (DAPI; Sigma; 1:1000). The entire culture plate was wrapped in foil and stored for overnight incubation at 4°C. The following day gels were rinsed with PBS (X3 for 5 min each) at room temperature and stored at 4°C until imaged.

Imaging was performed using an Olympus IX81 equipped with a Disc Spinning Unit and a 100 W high-pressure mercury burner (Olympus America), a Hamamatsu Orca II CCD camera (Hamamatsu Photonics; K.I.), and Metamorph Premier software (Molecular Devices). For vessel network formation, five images per construct were taken over a 200 μ m depth (10 slices at 20 μ m thick) at X4 magnification. Slices were superimposed using maximum intensity z-projection. Total network density was quantified using the Angiogenesis Tube Formation module in Metamorph Premier (Molecular Devices).

2.6 | Pericyte marker expression

VAS microtissues were harvested throughout preculture to assess the presence of pericyte markers and basement membrane proteins. After media removal and PBS rinse (X3 at 5 min each), microtissues were fixed in suspension with 2.0 ml Z-fix for 10 min at room temperature. Fixative

was removed and microtissues rinsed with PBS (X3 at 5 min each). Microtissues were then permeabilized with a 0.5% Triton X-100 solution in tris-buffered saline (TBS) for 30 min at 4°C and subsequently rinsed with 0.1% Triton X-100 in TBS (TBS_T, X3 for 5 min each). Microtissues were blocked overnight at 4°C with 2.0% bovine serum albumin (BSA; Sigma). After removal of blocking solution, microtissues were evenly split between five 1.5 ml Eppendorf tubes and incubated with 100 μ l appropriate primary antibody stain solution overnight at 4°C. Primary stain solutions comprised of TBS_T with 1.0% BSA (TBS_TBASA) containing: anti-alpha smooth muscle actin (1:200; abcam), antineural/glia antigen 2 (NG2; 1:200; abcam), antiplatelet-derived growth factor receptor- β (PDGFR- β ; 1:100; Sigma), anticollagen IV (1:500; ThermoFisher), or anti-laminin β (1:500; ThermoFisher). After incubation, primary antibody solution was removed and microtissues rinsed with TBS_T (X3 for 5 min each). Microtissues were then incubated with 100 μ l appropriate secondary antibody stain solution overnight at 4°C. Secondary stain solutions comprised of TBS_TBASA containing: goat anti-mouse (1:200; ThermoFisher) or goat anti-rabbit (1:500; ThermoFisher). After removal of secondary, microtissues were rinsed with TBS (X3 for 5 min each) and stored with TBS at 4°C until imaged. Imaging was performed using Olympus IX81 at X10 objective. Images were taken over a 300 μ m depth per microtissue (7 slices at 50 μ m thick). Slices were superimposed using maximum intensity z projection for qualitative analysis.

2.7 | Statistical analysis

Data are presented as mean \pm standard deviation ($n = 3$). Statistical significance was determined using two-way analysis of variance with a Tukey's multiple comparison post hoc test. All statistical analysis was performed using Prism 8.3 software (GraphPad). $p < 0.05$ was considered statistically significant.

3 | RESULTS

3.1 | Microtissue characterization

Characterization of vasculogenic (VAS) and osteogenic (OST) microtissues immediately after fabrication is shown in Figure 3. Microtissues exhibited a generally spheroidal morphology and remained as individual modules following emulsification and collection (Figure 3a). The batch emulsification process yielded a bell-shaped size distribution of microtissues (Figure 3b). The average diameter of VAS and OST microtissues were $220 \pm 9 \mu$ m and $180 \pm 13 \mu$ m, respectively. Homogeneously distributed viable cells were present in both types of microtissues following the fabrication and collection process (Figure 3c).

3.2 | Vasculogenic capacity of VAS microtissues

VAS microtissues were tested for the ability to support vascular network development in vitro, as shown in Figure 4. Microtissues

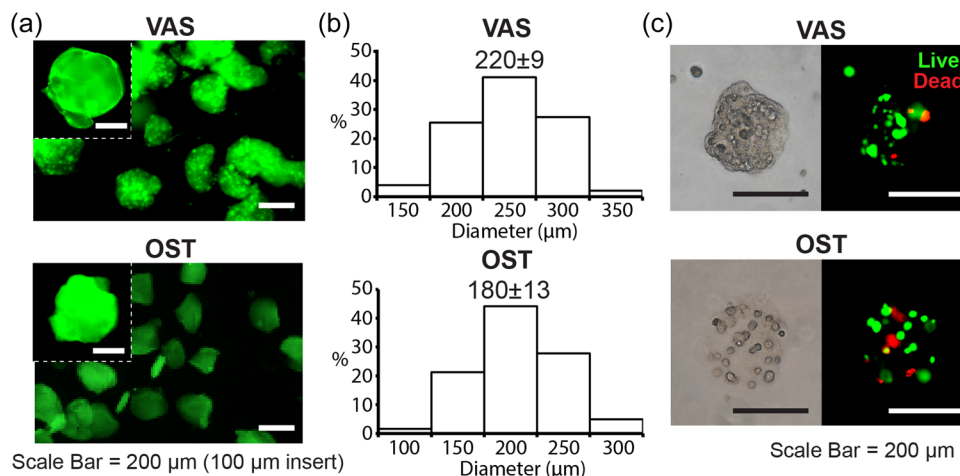


FIGURE 3 Characterization of microtissues. (a) Fluorescent images of FITC-labeled microtissues immediately following fabrication and collection. (b) Average size and size distribution of microtissues. (c) Brightfield (left panel) and fluorescent (right panel) images of microtissues revealing cellular distribution and viability (green = live cells, red = dead cells). OST, osteogenic; VAS, vasculogenic.

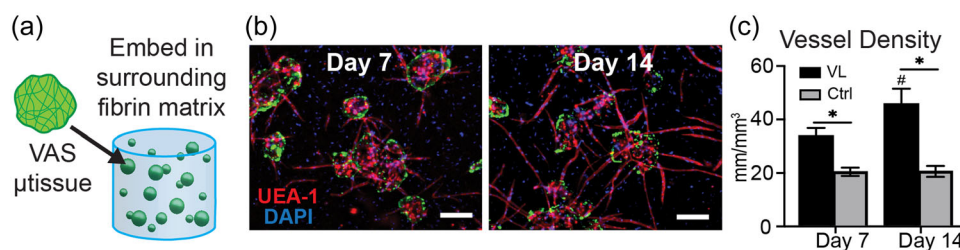


FIGURE 4 Vessel network formation by VAS microtissues. (a) Schematic of embedding of microtissues for vasculogenesis experiment. Microtissue-laden scaffolds cultured in either vasculogenic medium (VL) or control medium (Ctrl). (b) Confocal images of scaffolds cultured in VL revealing embedded microtissues (green), endothelial sprouts (red) and cell nuclei (blue). (c) Quantification of vessel density over time in culture ($n = 3$). Error bars represent standard deviation of the mean. #Indicates statistical significance compared to day 7 of the same condition ($p < 0.05$). *Indicates statistical significance between specified groups ($p < 0.05$). VAS, vasculogenic.

were embedded in a surrounding fibrin matrix to create solid gel constructs that kept the microtissues in place and supported vascular outgrowth throughout the culture period (Figure 4a). Confocal imaging revealed robust EC sprouting from microtissues into the surrounding matrix by 7 days of culture in vasculogenic medium (Figure 4b). Homogenous distribution of cellular nuclei lacking UEA-1 signal throughout the surrounding matrix suggests extensive MSC migration and/or proliferation from the embedded microtissues. EC sprouting had progressed by Day 14 of culture, forming primitive vessel-like networks through the surrounding matrix. Quantification of vessel density confirmed the qualitative observations. Constructs cultured in vasculogenic medium consistently displayed statistically significantly higher vessel densities compared to those cultured in control media (Figure 4c). Only constructs cultured in vasculogenic medium revealed an increase in network density over time.

3.3 | Osteogenic capacity of OST microtissues

Osteogenic(OST) microtissues were evaluated for the ability to support osteogenic differentiation in vitro, as shown in Figure 5. Microtissues were similarly embedded in a surrounding fibrin matrix to form a solid construct for culture (Figure 5a). Quantification of DNA content within constructs revealed a statistically significant increase in levels by Day 7, suggesting initial proliferative behavior of MSC (Figure 5b). Cell numbers remained stable over the second week of culture. Exposure to osteogenic supplements resulted in a decrease in ALP activity by Day 7, followed by a marked increase at Day 14 in osteogenically cultured constructs (Figure 5c). Constructs in control medium consistently displayed lower levels of ALP activity. Osteogenic culture resulted in progressive mineralization as noted by the significant increase in calcium mineral content within constructs throughout the culture period (Figure 5d).

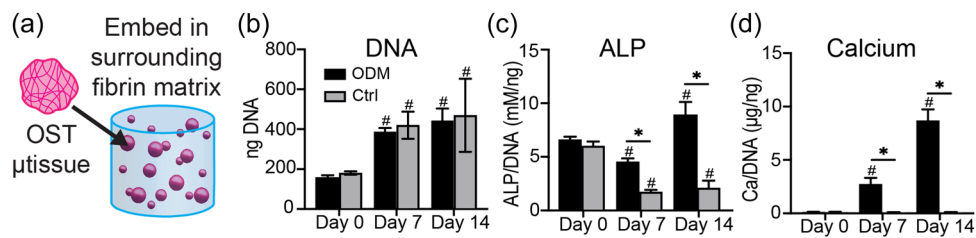


FIGURE 5 Osteogenic function of OST microtissues. (a) Schematic of embedding of microtissues for osteogenesis experiment. Microtissue-laden scaffolds cultured in either osteogenic differentiation medium (ODM) or control medium (Ctrl). Quantification of (b) DNA content, (c) alkaline phosphatase (ALP) activity, and (d) calcium mineral deposition over time in culture ($n = 3$). Error bars represent standard deviation of the mean. #Indicates statistical significance compared to Day 0 of the same condition ($p < 0.05$). *Indicates statistical significance between specified groups ($p < 0.05$).

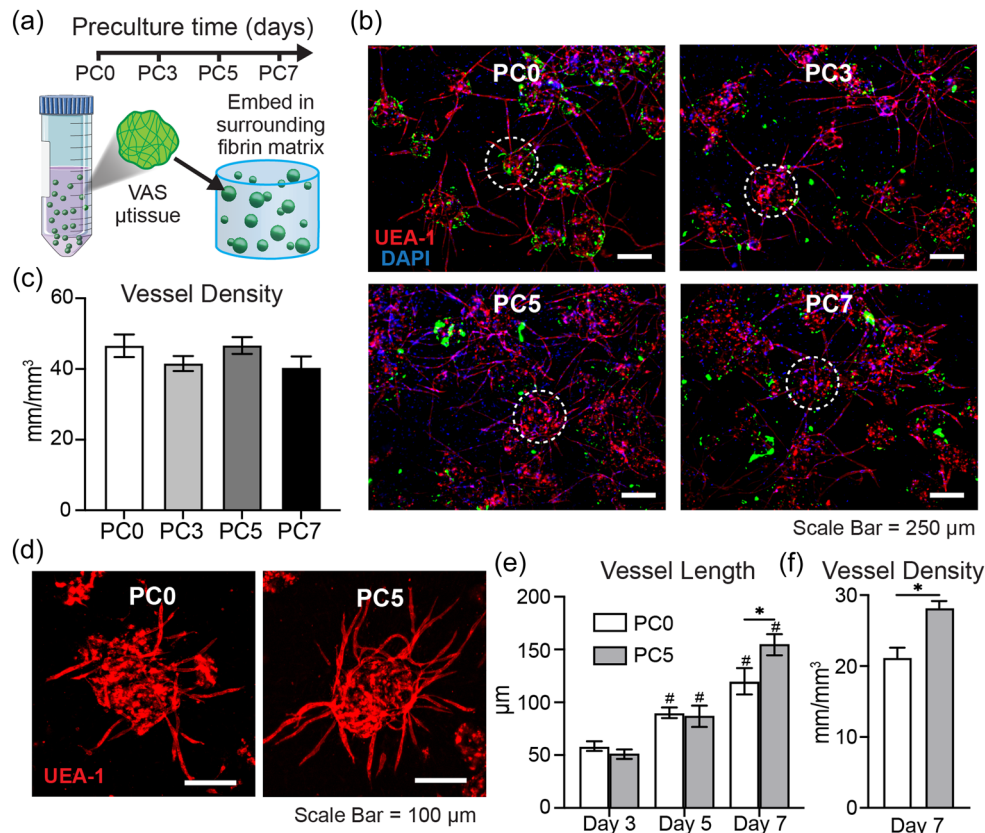


FIGURE 6 Effect of preculture on vessel network development by microtissues. (a) Schematic of preculture and embedding of microtissues for vasculogenesis experiment. Microtissues precultured for up to 7 days in suspension using vasculogenic medium before embedding in surrounding fibrin matrix. Constructs were then cultured for up to 14 days in vasculogenic medium to assess the influence of preculture time on vessel formation. PC# denotes microtissue preculture time in days. (b) Confocal images of microtissues after 14 days of culture in surrounding fibrin matrix revealing microtissue matrix (green), endothelial sprouts (red) and cell nuclei (blue). Dashed circle outlines embedded microtissues. (c) Quantification of vessel density at Day 14 ($n = 3$). (d) Confocal images of select microtissues at Day 7 of culture. Quantification of (e) vessel sprout length and (f) vessel density at specified time points throughout culture ($n = 3$). Error bars represent standard deviation of the mean. #Indicates statistical significance compared to Day 3 of the same condition ($p < 0.05$). *Indicates statistical significance between specified groups ($p < 0.05$).

3.4 | VAS microtissue preculture

VAS microtissues were precultured in suspension before embedding to investigate the effect of preculture time on their

vessel-forming potential, as shown in Figure 6. In these studies, microtissues were embedded in a surrounding fibrin matrix after 0, 3, 5, and 7 days of preculture, and the resultant constructs were subsequently cultured for up to 2 additional weeks

(Figure 6a). By the end of the culture period, all conditions supported the development of a robust vessel network distributed throughout the construct (Figure 6b). To differentiate microtissues from the surrounding fibrin matrix and to facilitate observation, the microtissues were labeled with a FITC marker that adhered only to the outer surface of fibrin. Interestingly, the stained layer on nonprecultured (P0) microtissues remained intact throughout the overall culture period, whereas constructs containing precultured microtissues exhibited stained fibrin fragments in the surrounding matrix. Quantification of formed networks revealed no statistical difference in vessel densities between conditions (Figure 6c). At 7 days of culture, EC sprouting appeared more extensive from microtissues that were precultured for 5 days compared to those that were not precultured (Figure 6d). Quantification of vessel sprout length (Figure 6e) and density (Figure 6f) confirmed this observation.

VAS microtissues were assessed for the ability to induce MSC pericyte-like lineage commitment through preculture, as shown in Figure 7. The presence of specific surface markers and basement

membrane proteins associated with vascular pericytes were qualitatively assessed in VAS microtissues throughout the 7-day preculture period (Figure 7a). (Loibl et al., 2014; Stratman & Davis, 2017) Following fabrication and collection, microtissues not exposed to preculture expressed very low levels of pericyte markers (Figure 7b). A slight increase in expression of α -smooth muscle actin, neuron-glia antigen 2, and PDGFR- β within microtissues was apparent by 3 days of preculture. By 5 days of preculture, microtissues displayed robust expression of all surface markers examined in addition to basement membrane proteins collagen IV and laminin. No clear enhancement in pericyte marker expression was observed at 7 days of preculture compared to Day 5. MSC morphology appeared spindle shaped within microtissues precultured for 5 days. Microtissues also contained multicellular EC structures resembling a primitive vascular plexus. This EC network appears to colocalize with basement membrane proteins and suggests MSC vascular lineage commitment through 5 days of preculture, as compared to no preculture.

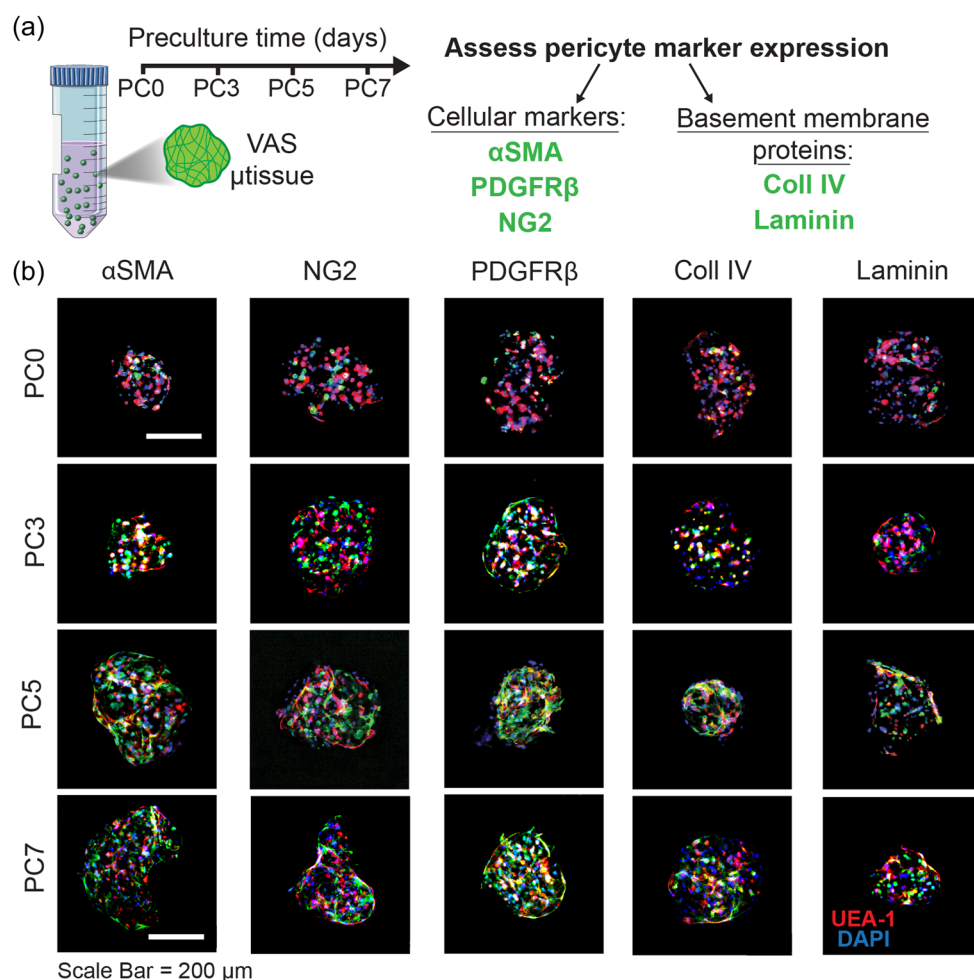


FIGURE 7 Pericyte lineage commitment as a function of preculture time. (a) Schematic of preculture experiment. (b) Confocal images of VAS microtissues throughout preculture revealing specific pericyte markers (green), endothelial cells (red), and cell nuclei (blue). VAS, vasculogenic.

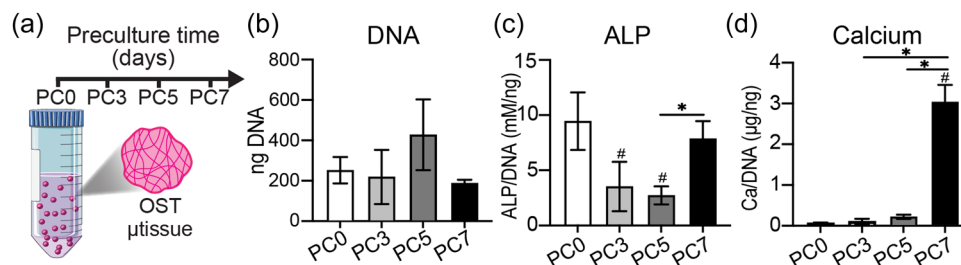


FIGURE 8 Effect of preculture on osteogenic lineage commitment in microtissues. (a) Schematic of preculture experiment. Microtissues were precultured for up to 7 days in suspension using osteogenic differentiation medium. Quantification of (b) DNA content, (c) ALP activity, and (d) calcium mineral deposition of OST microtissues throughout preculture ($n = 3$). PC# denotes microtissue preculture time (days). Error bars represent standard deviation of the mean. #Indicates statistical significance compared to no preculture ($p < 0.05$). *Indicates statistical significance between specified groups ($p < 0.05$). ALP, alkaline phosphatase.

3.5 | OST microtissue preculture

The ability of OST microtissues to support MSC osteogenic lineage commitment through preculture was investigated, as shown in Figure 8. Microtissues were quantitatively evaluated for specific osteogenic markers throughout the preculture period (Figure 8a). DNA quantification revealed no significant changes over 7 days of preculture (Figure 8b). ALP activity decreased over the first 3 days of preculture and remain stable until Day 5, followed by a significant increase in ALP activity at Day 7 of preculture (Figure 8c). Calcium mineral deposition within microtissues remained low over the first 5 days of preculture (Figure 8d). However, by Day 7 mineral content significantly increased suggesting osteogenic activity and MSC lineage commitment.

3.6 | Combination of OST and VAS microtissues in multimodular constructs

VAS and OST microtissues were evaluated for their ability to support osteogenic and vasculogenic development simultaneously, as shown in Figure 9. Both microtissue types were precultured to induce appropriate lineage commitment, and were then combined in a surrounding fibrin matrix to form a multimodular construct that was cultured for up to 14 days (Figure 9a). VAS microtissues that were precultured for 5 days were chosen for these studies because this was the shortest preculture time that supported robust pericyte marker expression. In addition, this preculture time was shown to enhance vessel sprout length and density in the surrounding fibrin matrix by 7 days of culture. OST microtissues that were precultured for 7 days were chosen, as this was the earliest time point shown to enhance osteogenic activity of MSC. Therefore, 5 and 7 days of microtissue preculture were deemed sufficient for inducing MSC vascular and osteogenic lineage commitment, respectively, and these microtissues were used for the generation of multimodular constructs.

Microscopic examination of multimodular constructs showed that they contained a relatively uniform distribution of both

microtissue types (Figure 9b). Precultured VAS (pVAS) microtissues supported the development of an extensive vessel-like network throughout the entire construct. Vessel density quantification revealed that constructs containing nonprecultured OST microtissues resulted in a significantly lower network density, compared to those containing pOST (Figure 9c). Quantification of osteogenic marker expression revealed enhanced ALP activity by Week 2 of culture, with no apparent effect of microtissue preculture (Figure 7d). Constructs containing both types of precultured microtissues as well as those in which only OST microtissues were precultured displayed a statistically significant increase in mineral deposition at Day 14, compared to those containing nonprecultured microtissues or those in which only VAS microtissues were precultured (Figure 9e). Histological evaluation revealed mineral deposition throughout pOST microtissues as well as in regions of the surrounding bulk matrix (Figure 9f).

4 | DISCUSSION

Despite progress in developing new MSC-based bone regeneration strategies, there remains an important need for achieving timely and sufficient vascularization to maintain appropriate cellular viability and function. Preforming vessel networks within constructs before transplantation has demonstrated promising effects by enhancing inosculation with host vasculature and overall neovascularization within the defect. (Chen et al., 2009; Roux et al., 2018) A rational approach to developing a vascularized bone construct involves exploiting the dual potential of MSC as both osteoprogenitors and as a vessel-supportive pericytes within a unified environment. Previous strategies have cocultured MSC and EC within biomaterial scaffold systems, while exposing them to a combination of osteoinductive and vasculogenic media components. However, these culture environments have been shown to have mutually incompatible effects on osteogenic differentiation and vessel development, demonstrating a need for alternative culture systems to achieve appropriate MSC phenotype and subsequent tissue development. Modular tissue engineering approaches, therefore

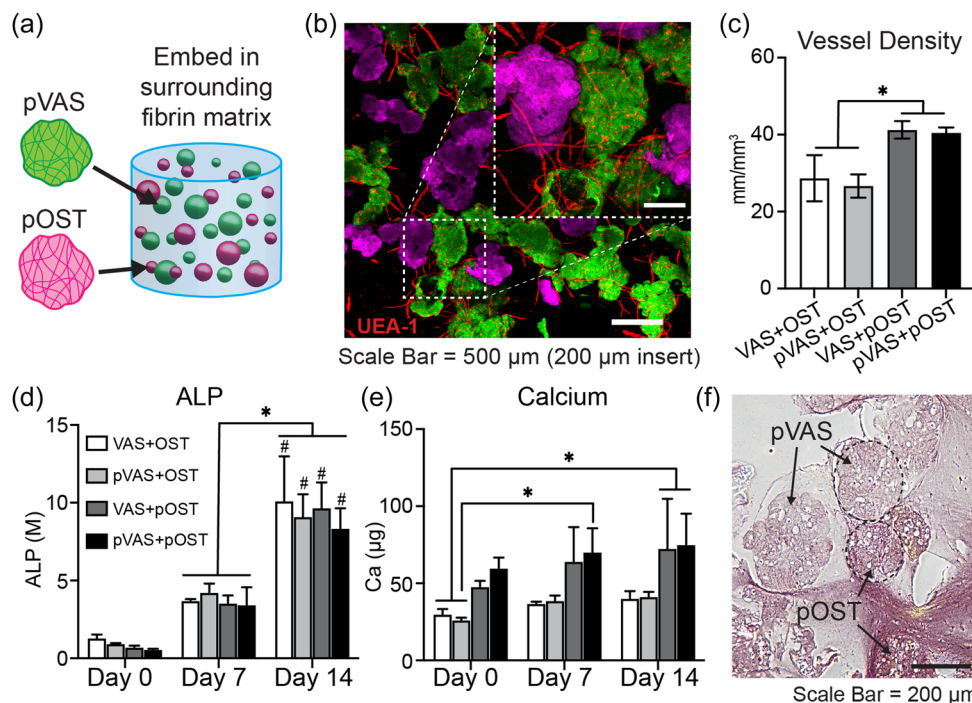


FIGURE 9 Multimodular construct containing precultured VAS and OST microtissues. (a) Schematic of embedding of precultured microtissues. (b) Confocal images of construct containing pVAS (green), pOST (purple), and vessel networks (red) after 14 days of culture. (c) Quantification of vessel density within constructs after 14 days of culture. Quantification of (d) ALP activity and (e) calcium mineral deposition within constructs over time in culture. (f) Alizarin red stain of construct after 14 days of culture. Error bars represent standard deviation of the mean ($n = 3$). #Indicates statistical significance compared to Day 0 of the same condition ($p < 0.05$). *Indicates statistical significance between specified groups ($p < 0.05$). ALP, alkaline phosphatase; OST, osteogenic; pOST, precultured osteogenic; pVAS, Precultured vasculogenic; VAS, vasculogenic.

have value in the generation of a vascularized bone construct by allowing separate control of culture conditions to induce desired phenotypes before their combination in a multimodular construct.

The goal of this study was to generate an MSC-based system capable of supporting concomitant vasculogenesis and osteogenesis as a proof-of-concept for the development of a vascularized bone construct. We employed a microtissue platform in which cells were encapsulated in modular biomaterial carriers tailored to support either a vasculogenic or osteogenic function. This microtissue platform has been previously explored in our lab and shown to support functional bone regeneration (Annamalai et al., 2019) and vessel development. (Friend et al., 2020) Here, separate populations of microtissues were generated and cultured under desired differentiation conditions to induce either an osteogenic or pericyte-like MSC phenotype. Preculture of OST microtissues enhanced osteogenesis by MSC and resulted in mineralization of the modular biomaterial carrier. Preculture of VAS microtissues supported the adoption of a pericyte-like phenotype, resulting in enhanced vascular sprouting. The modular nature of these precultured microtissues permitted subsequent combination to form a multimodular construct containing both osseous and vascular components. Importantly, this construct was capable of simultaneously supporting vessel development and osteogenic activity *in vitro* without the need for exogenous osteogenic supplements. These results suggest that separately

establishing MSC lineage commitment improves the simultaneous development of osseous and vascular components once combined. This approach provides an attractive means of inducing multiple MSC phenotypes under desired conditions while circumventing challenges with incompatible culturing environments.

The observed decrease in vessel density within constructs containing nonprecultured OST microtissues may be a result of the presence of undifferentiated MSC, which have been shown to exhibit antiangiogenic effects through paracrine pathways involving soluble factors, including IL-10, TGF β , and IL-6. (Eslani et al., 2017; Ho et al., 2013; Oh et al., 2008) In the current study, preculture of OST microtissues was used to induce osteogenic lineage commitment, which also is likely to have changed the secretory profile of MSC in such a way as to avoid the inhibition of neovascularization. Interestingly, this inhibitory effect was observed only with non-precultured OST microtissues, and not VAS microtissues. Unlike OST microtissues, VAS microtissues contain EC that may provide a direct cellular stimulus to induce MSC pericyte-like differentiation. (Loibl et al., 2014) This direct cellular cue and the biochemical factors in the vasculogenic media used to culture multimodular constructs likely induce pericyte-like lineage commitment in MSC, and thereby avoid the inhibitive effect of undifferentiated MSC on *in vitro* vessel development. This finding emphasizes the importance of preconditioning of MSC to induce appropriate lineage commitment, as well as

the use of the appropriate microtissue platform to achieve a desired phenotype. Previous MSC preconditioning strategies have been shown to influence MSC paracrine signaling, enhance cell survival, and proliferation. (Pasha et al., 2008; Waszak et al., 2012)

The presence of OST microtissues enhanced osteogenic activity in multimodular constructs. Regardless of preculture regimen, a sustained increase in ALP activity was apparent in all construct conditions, which is generally accepted as an early-stage osteogenic marker and has been shown to accurately predict *in vivo* bone forming ability. (Prins et al., 2014) Preculture of OST microtissues resulted in osteogenic lineage commitment, as further demonstrated by increased mineral deposition by multimodular constructs over time, as compared to those containing nonprecultured OST microtissues. This observation was particularly interesting since the constructs were cultured in a vasculogenic medium, which has been shown in other studies to directly impair the mineralization capacity of MSC (Kolbe et al., 2011; Schott & Stegemann, 2021) It is possible that this inhibitory effect is most prominent when MSC have an undifferentiated phenotype, which would explain why precultured OST microtissues containing MSC with established lineage commitment displayed better performance. Preculture was also shown to support mineralization within OST microtissues, which has been shown to have an osteoinductive effect on MSC. (Wu et al., 2021) Mineral deposition occurred throughout the precultured OST microtissues as well as in the surrounding matrix, suggesting osteogenic activity taking place outside of the microtissues themselves. The presence of deposited mineral in the matrix during the preculture phase may have created an environment permissive to subsequent osteogenic activity and sustained mineralization.

Modular tissue engineering strategies have advantages that are important in moving the field toward the creation of clinically-relevant engineered tissues for human implantation. (Amini & Nair, 2012; Nichol & Khademhosseini, 2009) The multimodular approach described here offers a unique ability to independently control microenvironmental cues that direct cellular function. This study leveraged the ability to separately induce osteogenic and vasculogenic phenotypic commitment in MSC, while circumventing the challenge of using incompatible culture media. The combined culture of these microtissue components was found to enable concomitant vessel and osteogenic development within a unified system, thereby demonstrating an attractive platform for the development of a vascularized bone construct.

5 | CONCLUSION

The current study introduces a modular approach in which MSC-laden microtissues can be separately precultured under defined conditions to induce appropriate lineage commitment, and are subsequently combined to form a dual-phase construct. The findings highlight the importance of MSC phenotype in coupling

vasculogenesis and osteogenesis within a unified system. Osteogenic preculture of MSC within microtissues enabled sustained osteogenic activity even when cultured in a vasculogenic environment, thereby eliminating the need for exogenous osteoinductive factors that may compromise vessel development. This study also reveals a means of inducing a pericyte-like phenotype in MSC and resulting nascent blood vessels in microtissues, which can then be combined with other tissue types without disrupting the surrounding matrix. This approach could be used for incorporating a vascular component into a range of tissue types where rapid establishment of a vascular supply is needed for successful transplantation. Taken together, this study shows that microtissues can be used to exploit the dual-differentiation potential of MSC to support simultaneous vessel development and osteogenic differentiation in a proof-of-concept approach for the development of vascularized engineered bone.

ACKNOWLEDGMENT

This study was supported in part by the National Institute of Arthritis and Musculoskeletal and Skin Diseases (R01-AR062636, to JPS). NGS is partially supported by the Cellular Biotechnology Training Program (T32-GM008353) at the University of Michigan. The content is solely the responsibility of the authors and does not necessarily represent the official views of the National Institutes of Health. Some of the figures in this article were created using Servier Medical Art templates, and are licensed under a Creative Commons Attribution 3.0 Unported License (smart.servier.com).

CONFLICT OF INTEREST

The authors declare no conflict of interest.

DATA AVAILABILITY STATEMENT

The data that support the findings of this study are available from the corresponding author upon reasonable request.

ORCID

Nicholas G. Schott  <http://orcid.org/0000-0003-4344-0818>

REFERENCES

- Amini, A. A., & Nair, L. S. (2012). Injectable hydrogels for bone and cartilage repair. *Biomedical Materials*, 7(2), 024105. <https://doi.org/10.1088/1748-6041/7/2/024105>
- Annamalai, R. T., Hong, X., Schott, N. G., Tiruchinapally, G., Levi, B., & Stegemann, J. P. (2019). Injectable osteogenic microtissues containing mesenchymal stromal cells conformally fill and repair critical-size defects. *Biomaterials*, 208, 32–44. <https://doi.org/10.1016/j.biomaterials.2019.04.001>
- Barrère, F., Mahmood, T. A., de Groot, K., & van Blitterswijk, C. A. (2008). Advanced biomaterials for skeletal tissue regeneration: Instructive and smart functions. *Materials Science and Engineering R: Reports*, 59(1–6), 38–71. <https://doi.org/10.1016/j.mser.2007.12.001>
- Carrion, B., Janson, I. A., Kong, Y. P., & Putnam, A. J. (2014). A safe and efficient method to retrieve mesenchymal stem cells from three-dimensional fibrin gels. *Tissue Engineering. Part C, Methods*, 20(3), 252–263. <https://doi.org/10.1089/ten.TEC.2013.0051>
- Chen, X., Aledia, A. S., Ghajar, C. M., Griffith, C. K., Putnam, A. J., Hughes, C. C. W., & George, S. C. (2009). Prevascularization of a

- fibrin-based tissue construct accelerates the formation of functional anastomosis with host vasculature. *Tissue Engineering - Part A*, 15(6), 1363–1371. <https://doi.org/10.1089/ten.tea.2008.0314>
- Chiesa, I., De Maria, C., Lapomarda, A., Fortunato, G. M., Montemurro, F., Di Gesù, R., Tuan, R. S., Vozi, G., & Gottardi, R. (2020). Endothelial cells support osteogenesis in an in vitro vascularized bone model developed by 3D bioprinting. *Biofabrication*, 12(1), 025013. <https://doi.org/10.1088/1758-5090/ab6a1d>
- Correia, C., Grayson, W., Eton, R., Gimble, J. M., Sousa, R. A., Reis, R. L., & Vunjak-Novakovic, G. (2014). Human adipose-derived cells can serve as a single-cell source for the in vitro cultivation of vascularized bone grafts. *Journal of Tissue Engineering and Regenerative Medicine*, 8, 629–639. <https://doi.org/10.1002/term>
- Dimitriou, R., Mataliotakis, G. I., Angoules, A. G., Kanakaris, N. K., & Giannoudis, P. V. (2011). Complications following autologous bone graft harvesting from the iliac crest and using the RIA: A systematic review. *Injury*, 42(Suppl 2), S3–S15. <https://doi.org/10.1016/j.injury.2011.06.015>
- Eslani, M., Putra, I., Shen, X., Hamouie, J., Afsharkhamesh, N., Besharat, S., Rosenblatt, M. I., Dana, R., Hematti, P., & Djalilian, A. R. (2017). Corneal mesenchymal stromal cells are directly antiangiogenic via PEDF and sFLT-1. *Investigative Ophthalmology and Visual Science*, 58(12), 5507–5517. <https://doi.org/10.1167/iov.17-22680>
- Forrestal, D. P., Klein, T. J., & Woodruff, M. A. (2017). Challenges in engineering large customized bone constructs. *Biotechnology and Bioengineering*, 114(6), 1129–1139. <https://doi.org/10.1002/bit.26222>
- Friend, N. E., Rioja, A. Y., Kong, Y. P., Beamish, J. A., Hong, X., Habif, J. C., Bezenah, J. R., Deng, C. X., Stegemann, J. P., & Putnam, A. J. (2020). Injectable pre-cultured tissue modules catalyze the formation of extensive functional microvasculature in vivo. *Scientific Reports*, 10(1), 1–16. <https://doi.org/10.1038/s41598-020-72576-5>
- Ho, I. A. W., Toh, H. C., Ng, W. H., Teo, Y. L., Guo, C. M., Hui, K. M., & Lam, P. Y. P. (2013). Human bone marrow-derived mesenchymal stem cells suppress human glioma growth through inhibition of angiogenesis. *Stem Cells*, 31(1), 146–155. <https://doi.org/10.1002/stem.1247>
- Ho-Shui-Ling, A., Bolander, J., Rustom, L. E., Johnson, A. W., Luyten, F. P., & Picart, C. (2018). Bone regeneration strategies: Engineered scaffolds, bioactive molecules and stem cells current stage and future perspectives. *Biomaterials*, 180, 143–162. <https://doi.org/10.1016/j.biomaterials.2018.07.017>
- Hutton, D. L., Moore, E. M., Gimble, J. M., & Grayson, W. L. (2013). Platelet-Derived growth factor and spatiotemporal cues induce development of vascularized bone tissue by Adipose-Derived stem cells. *Tissue Engineering. Part A*, 19(17–18), 2076–2086. <https://doi.org/10.1089/ten.tea.2012.0752>
- Jaiswal, N., Haynesworth, S. E., Caplan, A. I., & Bruder, S. P. (1997). Osteogenic differentiation of purified, culture-expanded human mesenchymal stem cells in vitro. *Journal of Cellular Biochemistry*, 64(2), 295–312.
- Kolbe, M., Xiang, Z., Dohle, E., Tonak, M., Kirkpatrick, C. J., & Fuchs, S. (2011). Paracrine effects influenced by cell culture medium and consequences on microvessel-like structures in cocultures of mesenchymal stem cells and outgrowth endothelial cells. *Tissue Engineering - Part A*, 17(17–18), 2199–2212. <https://doi.org/10.1089/ten.tea.2010.0474>
- Laurencin, C., Khan, Y., & El-Amin, S. F. (2006). Bone graft substitutes. *Expert Review of Medical Devices*, 3(1), 49–57. <https://doi.org/10.1586/17434440.3.1.49>
- Loibl, M., Binder, A., Herrmann, M., Duttonhoefer, F., Richards, R. G., Nerlich, M., Alini, M., & Verrier, S. (2014). Direct cell-cell contact between mesenchymal stem cells and endothelial progenitor cells induces a pericyte-like phenotype in vitro. *BioMed Research International*, 2013, 1–10. <https://doi.org/10.1155/2014/395781>
- Mishra, R., Roux, B. M., Posukonis, M., Bodamer, E., Brey, E. M., Fisher, J. P., & Dean, D. (2016). Effect of prevascularization on in vivo vascularization of poly(propylene fumarate)/fibrin scaffolds. *Biomaterials*, 77, 255–266. <https://doi.org/10.1016/j.biomaterials.2015.10.026>
- Nichol, J. W., & Khademhosseini, A. (2009). Modular tissue engineering: Engineering biological tissues from the bottom up. *Soft Matter*, 5(7), 1312–1319. <https://doi.org/10.1039/b814285h>
- Novosel, E. C., Kleinhans, C., & Kluger, P. J. (2011). Vascularization is the key challenge in tissue engineering. *Advanced Drug Delivery Reviews*, 63(4), 300–311. <https://doi.org/10.1016/j.addr.2011.03.004>
- Oh, J. Y., Kim, M. K., Shin, M. S., Lee, H. J., Ko, J. H., Wee, W. R., & Lee, J. H. (2008). The anti-inflammatory and anti-angiogenic role of mesenchymal stem cells in corneal wound healing following chemical injury. *Stem Cells*, 26(4), 1047–1055. <https://doi.org/10.1634/stemcells.2007-0737>
- Oryan, A., Kamali, A., Moshiri, A., & Eslaminejad, M. B. (2017). Role of mesenchymal stem cells in bone regenerative Medicine: what is the evidence. *Cells Tissues Organs*, 204, 59–83. <https://doi.org/10.1159/000469704>
- Pasha, Z., Wang, Y., Sheikh, R., Zhang, D., Zhao, T., & Ashraf, M. (2008). Preconditioning enhances cell survival and differentiation of stem cells during transplantation in infarcted myocardium. *Cardiovascular Research*, 77(1), 134–142. <https://doi.org/10.1093/cvr/cvm025>
- Perry, L., Merdler, U., Elishaev, M., & Levenberg, S. (2019). Enhanced host neovascularization of prevascularized engineered muscle following transplantation into immunocompetent versus immunocompromised mice. *Cells*, 8, 1472–1488.
- Prins, H. J., Braat, A. K., Gawlitta, D., Dhert, W. J., Egan, D. A., Tijssen-Slump, E., Yuan, H., Coffey, P. J., Rozemuller, H., & Martens, A. C. (2014). In vitro induction of alkaline phosphatase levels predicts in vivo bone forming capacity of human bone marrow stromal cells. *Stem Cell Research*, 12(2), 428–440. <https://doi.org/10.1016/j.scr.2013.12.001>
- Rao, R. R., Vigen, M. L., Peterson, A. W., Caldwell, D. J., Putnam, A. J., & Stegemann, J. P. (2015). Dual-phase osteogenic and vasculogenic engineered tissue for bone formation. *Tissue Engineering. Part A*, 21(3–4), 530–540. <https://doi.org/10.1089/ten.tea.2013.0740>
- Rohringer, S., Hofbauer, P., Schneider, K. H., Husa, A. M., Feichtinger, G., Peterbauer-Scherb, A., Redl, H., & Holthöner, W. (2014). Mechanisms of vasculogenesis in 3D fibrin matrices mediated by the interaction of adipose-derived stem cells and endothelial cells. *Angiogenesis*, 17(4), 921–933. <https://doi.org/10.1007/s10456-014-9439-0>
- Roux, B. M., Akar, B., Zhou, W., Stojkova, K., Barrera, B., Brankov, J., & Brey, E. M. (2018). Preformed vascular networks survive and enhance vascularization in critical sized cranial defects. *Tissue Engineering - Part A*, 24(21–22), 1603–1615. <https://doi.org/10.1089/ten.tea.2017.0493>
- Santos, T. S., Abuna, R. P. F., Castro Raucchi, L. M. S., Teixeira, L. N., De Oliveira, P. T., Beloti, M. M., & Rosa, A. L. (2015). Mesenchymal stem cells repress osteoblast differentiation under osteogenic-inducing conditions. *Journal of Cellular Biochemistry*, 116(12), 2896–2902. <https://doi.org/10.1002/jcb.25237>
- Schott, N. G., Friend, N. E., & Stegemann, J. P. (2021). Coupling osteogenesis and vasculogenesis in engineered orthopedic tissues. *Tissue Engineering Part B: Reviews*, 27(3), 199–214. <https://doi.org/10.1089/ten.teb.2020.0132>
- Schott, N. G., & Stegemann, J. P. (2021). Coculture of endothelial and stromal cells to promote concurrent osteogenesis and vasculogenesis. *Tissue Engineering. Part A*, 27(21–22), 1376–1386. <https://doi.org/10.1089/ten.tea.2020.0330>
- Sears, V., & Ghosh, G. (2020). Harnessing mesenchymal stem cell secretome: effect of extracellular matrices on pro-angiogenic signaling. *Biotechnology and Bioengineering*, 117, 1159–1171. <https://doi.org/10.1002/bit.27272>

- Shoulders, M. D., & Raines, R. T. (2009). Collagen structure and stability. *Annual Review of Biochemistry*, 78, 929–958. <https://doi.org/10.1146/annurev.biochem.77.032207.120833>
- Stapor, P. C., Sweat, R. S., Dashti, D. C., Betancourt, A. M., & Murfee, W. L. (2014). Pericyte dynamics during angiogenesis: New insights from new identities. *Journal of Vascular Research*, 51(3), 163–174. <https://doi.org/10.1159/000362276>
- Stratman, A. N., & Davis, G. E. (2017). Endothelial cell-pericyte interactions stimulate basement membrane matrix assembly: Influence on vascular tube. *Microscopy and Microanalysis: The Official Journal of Microscopy Society of America, Microbeam Analysis Society, Microscopical Society of Canada*, 18(1), 68–80.
- Vater, C., Kasten, P., & Stiehler, M. (2011). Culture media for the differentiation of mesenchymal stromal cells. *Acta Biomaterialia*, 7(2), 463–477. <https://doi.org/10.1016/j.actbio.2010.07.037>
- Waszak, P., Alphonse, R., Vadivel, A., Ionescu, L., Eaton, F., & Thébaud, B. (2012). Preconditioning enhances the paracrine effect of mesenchymal stem cells in preventing oxygen-induced neonatal lung injury in rats. *Stem Cells and Development*, 21(15), 2789–2797. <https://doi.org/10.1089/scd.2010.0566>
- Wenz, A., Tjoeng, I., Schneider, I., Kluger, P. J., & Borchers, K. (2018). Improved vasculogenesis and bone matrix formation through coculture of endothelial cells and stem cells in tissue-specific methacryloyl gelatin-based hydrogels. *Biotechnology and Bioengineering*, 115(10), 2643–2653. <https://doi.org/10.1002/bit.26792>
- Wise, J. K., Alford, A. I., Goldstein, A. S., & Stegemann, J. P. (2016). Synergistic enhancement of ectopic bone formation by supplementation of freshly isolated marrow cells with purified MSC in collagen–chitosan hydrogel microbeads. *Connective Tissue Research*, 57(6), 516–525. <https://doi.org/10.1016/j.physbeh.2017.03.040>
- Wu, X., Walsh, K., Suvarnapathaki, S., Lantigua, D., McCarthy, C., & Camci-Unal, G. (2021). Mineralized paper scaffolds for bone tissue engineering. *Biotechnology and Bioengineering*, 118(3), 1411–1418. <https://doi.org/10.1002/bit.27652>
- Ye, X., Yin, X., Yang, D., Tan, J., & Liu, G. (2012). Ectopic bone regeneration by human bone marrow mononucleated cells, undifferentiated and osteogenically differentiated bone marrow mesenchymal stem cells in beta-tricalcium phosphate scaffolds. *Tissue Engineering - Part C: Methods*, 18(7), 545–556. <https://doi.org/10.1089/ten.tec.2011.0470>

How to cite this article: Schott, N. G., Vu, H., & Stegemann, J. P. (2022). Multimodular vascularized bone construct comprised of vasculogenic and osteogenic microtissues. *Biotechnology and Bioengineering*, 119, 3284–3296. <https://doi.org/10.1002/bit.28201>